

Noise Dephasing in Edge States of the Integer Quantum Hall Regime

P. Roulleau, F. Portier, and P. Roche

CEA Saclay, Service de Physique de l'Etat Condensé, Nanoelectronic Group, F-91191 Gif-sur-Yvette, France

A. Cavanna, G. Faini, U. Gennser, and D. Mailly

CNRS, Laboratoire de Photonique et Nanostructures, Phynano team, Route de Nozay, F-91460 Marcoussis, France

(Received 15 February 2008; published 29 October 2008)

An electronic Mach-Zehnder interferometer is used in the integer quantum Hall regime at a filling factor 2 to study the dephasing of the interferences. This is found to be induced by the electrical noise existing in the edge states capacitively coupled to each other. Electrical shot noise created in one channel leads to phase randomization in the other, which destroys the interference pattern. These findings are extended to the dephasing induced by thermal noise instead of shot noise: it explains the underlying mechanism responsible for the finite temperature coherence time $\tau_\varphi(T)$ of the edge states at filling factor 2, measured in a recent experiment. Finally, we present here a theory of the dephasing based on Gaussian noise, which is found to be in excellent agreement with our experimental results.

DOI: 10.1103/PhysRevLett.101.186803

PACS numbers: 73.43.Fj, 03.65.Yz, 73.23.Ad

Although many experiments in quantum optics can be reproduced with electron beams using the edge states of the Integer Quantum Hall Effect (IQHE), there exist fundamental differences due to the Coulomb interaction. As an example, the Mach-Zehnder type of interferometer in the IQHE [1] has recently allowed us to observe quantum interferences with the unprecedented 90% visibility [2], opening a new field of promising quantum information experiments. Indeed, the edge states of the IQHE provide a way to obtain “ideal” unidimensional quantum wires. However, very little is known about the decoherence processes in these “ideal” wires. Only very recently has their coherence length been quantitatively determined as well as its temperature dependence established [3]. Here, we show that the underlying mechanism responsible for the finite coherence length is the thermal noise combined with the poor screening in the IQHE regime [4].

In the IQHE, gapless excitations develop on the edge of the sample and form one dimensional chiral wires (edge states), the number of which is determined by the number of electrons per quantum of flux (the filling factor ν). In these wires, the electrons drift along the edge in a beamlike motion making experiments usually done with photons possible with electrons. The choice of the filling factor at which one obtains high visibility interferences requires a compromise between a magnetic field high enough to form well-defined edge states, and small enough to still deal with a good Fermi liquid. Naïvely, one could think that the highest visibility would have been observed at $\nu = 1$, but it is not actually the case [1]. This may be due to decoherence induced by collective spin excitations (Skyrmions [5]) making spin flip processes possible. In practice, the highest visibility (90% [2]) has been obtained at filling factor 2, when there are two spin polarized edge states. Here, chirality and unidimensionality prevent first order inelastic

scattering in the wires themselves [6], while tunneling from one edge to the other requires spin flip [7].

To show that the origin of the finite coherence length is related to the coupling between two neighboring edge states, we have proceeded as follow. First, we have made a which-path experiment inducing on-purpose shot noise on the inner edge state (IES) while measuring the outer edge state (OIS) interferences. The visibility decrease is shown to result from a Gaussian noise, in opposition to a recent experiment [8]. Using the parameters extracted from the which-path measurements, we are able to calculate the dephasing resulting from thermal noise (instead of shot noise). The result is in perfect agreement with our recent measurements of the finite temperature coherence length [9]. Moreover, the magnetic field dependence of the coherence length is shown to result from a variation of the coupling between the two edges. Finally, we have developed a theory which gives a full scheme of the dephasing mediated by the electronic noise.

The interferences are obtained using an electronic Mach-Zehnder Interferometer (MZI) which was patterned on a high mobility two dimensional electron gas at a GaAs/Ga_{1-x}Al_xAs heterojunction (density $n_S = 2.0 \times 10^{11} \text{ cm}^{-2}$ and mobility $\mu = 2.5 \times 10^6 \text{ cm}^2/\text{Vs}$). Measurements have been done in the quantum Hall regime, at filling factor 2 (with a magnetic field $B \sim 4.5 \text{ T}$). In the edge states, the electrons have a chiral motion with a drift velocity of the order of $10^4\text{--}10^5 \text{ ms}^{-1}$. A SEM view of the sample as well as a schematic representation of the two edge states are shown in Fig. 1(a). The outer incoming edge state is split by $G1$ in two paths (a) and (b), which are recombined at $G2$ leading to interferences. SG is a side gate used to change the area S defined by the two arms of the interferometer. The current which is not transmitted through the MZ, $I_R = I_0 - I_T$, is collected to the ground

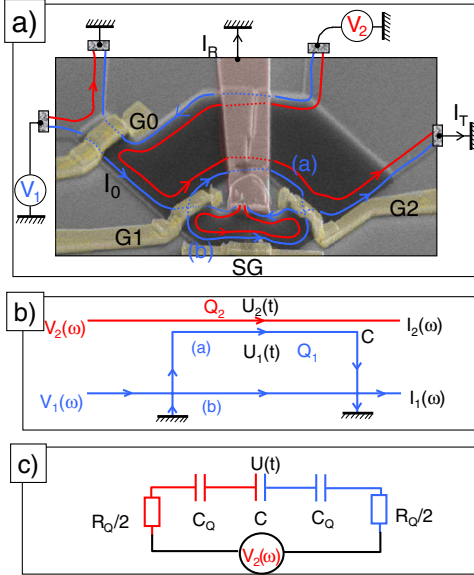


FIG. 1 (color online). (a) Tilted SEM view of the device, with schematic representation of the edge states. $G1$ and $G2$ are Quantum Point Contact (QPC) which define the two beam splitters of the Mach-Zehnder interferometer. They are set to transmission $\mathcal{T}_1 \sim \mathcal{T}_2 \sim 1/2$ for the OES, while fully reflecting the IES. The two arms (a) and (b) are $L = 11.3 \mu\text{m}$ long defining an area S of $34 \mu\text{m}^2$. The small inner Ohmic contact is connected to the ground via an Au metallic bridge. SG is a side gate. $G0$ is an additional beam splitter which makes it possible to bias the IES by V_2 , while the other is biased by V_1 . $G0$ is tuned such that the OES is fully reflected, while the IES is transmitted with a probability \mathcal{T}_0 . (b) Schematic representation of the edge states coupled by a geometrical capacitance C . (c) Low frequency equivalent circuit with V_1 set to 0 V, $C_Q = \tau/R_Q$.

via the inner Ohmic contact. The differential transmission $\mathcal{T} = dI_T/dI_0$ have been measured at low temperature (~ 20 mK) by standard lock-in techniques with an ac voltage ($V_1 \sim 1 \mu\text{V}_{\text{RMS}}$ at 619 Hz).

It is straightforward to show that $\mathcal{T} \propto [1 + \mathcal{V} \sin(\varphi)]$, \mathcal{V} being the visibility and φ the Aharonov-Bohm (AB) flux through S [9]. In the present study, we tuned the transmission \mathcal{T}_1 and \mathcal{T}_2 of the beam splitters $G1$ and $G2$ to $1/2$ in order to have a maximum visibility. The interferences are revealed by varying φ . It can be done either by applying a voltage V_{SG} on the side gate, or by applying a voltage V_2 on the IES (playing here a role similar to the side gate). In Fig. 2, we have plotted the interference pattern obtained by the two methods. The periodicity V_0 of interferences with respect to V_2 depends on the coupling between the two edge states which will be shown to be related to the time of flights through the MZI. In Fig. 4, one can notice that V_0 exhibits a large non-monotonic variation with the magnetic field on the Hall plateau at $\nu = 2$.

Any fluctuations on V_2 blur the phase. For a Gaussian distribution of the phase (we will discuss this notion later), the visibility is proportional to $e^{-(\delta\varphi^2)/2}$ [10] where $\langle \delta\varphi^2 \rangle$

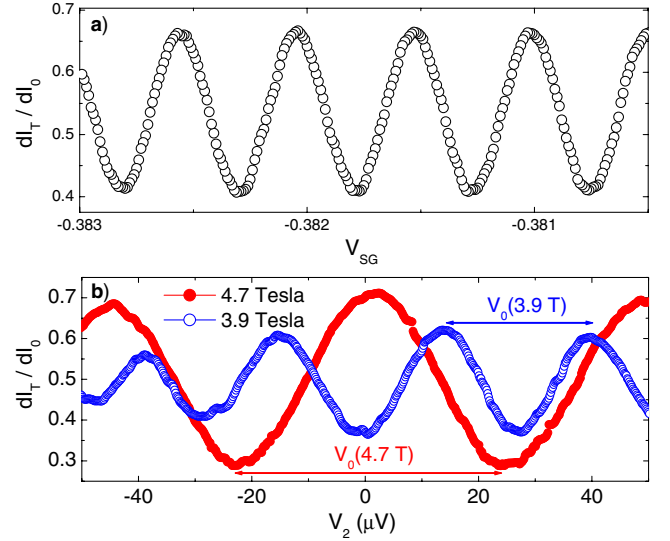


FIG. 2 (color online). (a) Phase sweeping by varying the side gate voltage V_{SG} . (b) Phase sweeping by varying V_2 with $\mathcal{T}_0 = 1$ for two different magnetic fields. The periodicity V_0 depends on the magnetic field as shown in Fig. 4.

is the variance of the Gaussian distribution. It is simply related to the noise power spectrum S_{22} of V_2 through the coupling constant and the (unknown) bandwidth $\Delta\nu$: $\langle \delta\varphi^2 \rangle = (2\pi)^2 \langle \delta V_2^2 \rangle / V_0^2 = (2\pi)^2 S_{22} \Delta\nu / V_0^2$. If one generates partition noise on the IES tanks to the splitter G_0 , the resulting excess noise $\Delta S_{22} = 2eR_Q \mathcal{T}_0 (1 - \mathcal{T}_0) V_2 \{ \coth[eV_2/(2k_B T)] - 2k_B T / (eV_2) \}$ [11,12] leads to a visibility decreasing exponentially with V_2 when $eV_2 \gg k_B T$:

$$\mathcal{V} = \mathcal{V}_0(T) e^{-\mathcal{T}_0(1-\mathcal{T}_0)(V_2 - 2k_B T/e)/V_\varphi}, \quad (1)$$

$$\text{with } V_\varphi^{-1} = \frac{4\pi^2 e R_Q}{V_0^2} \Delta\nu, \quad (2)$$

and $R_Q = 1/G_Q = h/e^2$.

In Eq. (1), the unknown parameter is V_φ which is related to the bandwidth $\Delta\nu$ [Eq. (2)]. This approach for the dephasing is valid only if $\Delta\nu$ is such that the fluctuations lead to a Gaussian distribution of φ . It implies that many electrons have to be involved in the dephasing during the measuring time $1/\Delta\nu$, namely, that $\max(eV_2, 2k_B T) \gg h\Delta\nu$. This condition coincides with the fact that the noise power spectrum S_{22} can be considered as frequency independent. Note that the dephasing rate increases with V_2 because the number of involved electrons increases, not because the coupling between electrons increases with V_2 (as claimed in [8]). Figure 3 shows that our data are in remarkable agreement with Eq. (2). In Fig. 3(a), we have plotted the visibility versus V_2 when $\mathcal{T}_0 = 1/2$, for two different magnetic fields. \mathcal{V} decreases exponentially with V_2 . The solid lines are fits to the data using an electronic temperature of 25 mK (for a fridge temperature of 20 mK).

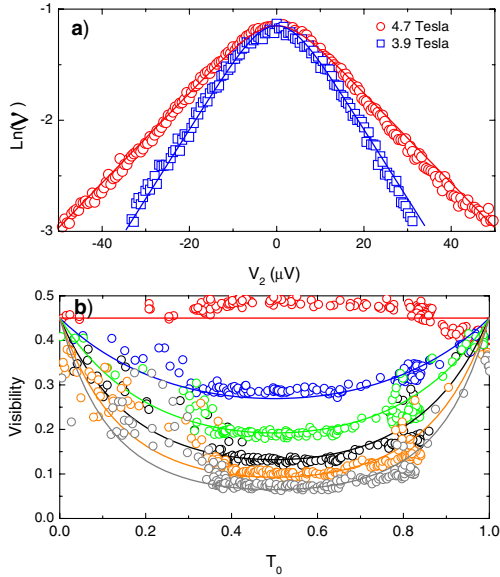


FIG. 3 (color online). (a) Visibility decrease of the interferometer as a function of V_2 at $\mathcal{T}_0 = 1/2$ for two different magnetic fields 4.7 and 3.9 T. The solid lines are fit to the data $\mathcal{V} = \mathcal{V}_0 e^{-2\pi^2 \Delta S_{22} \Delta \nu / V_0^2}$ with an electronic temperature of 25 mK (for a base temperature of 20 mK) and $\mathcal{T}_0 = 1/2$. The high bias fit of the exponential decrease $\mathcal{V} = \mathcal{V}_0 \exp[-\mathcal{T}_0(1 - \mathcal{T}_0)V_2/V_\phi]$ allows us to determine V_ϕ which is found to depend on the magnetic field. (b) Visibility decrease of the interferometer as a function of \mathcal{T}_0 for $V_2 = 0, 21, 31, 42, 53,$ and $63 \mu\text{V}$ from top to bottom. The solid lines are fits to the data using Eq. (1) with $\mathcal{V}_0 = 0.45$, $V_\phi = 7.2 \mu\text{V}$, and $T = 25 \text{ mK}$.

V_ϕ and \mathcal{V}_0 are the fitting parameters. The values of V_ϕ deduced from these measurements depend on the magnetic field in the same way as V_0 . In fact, V_ϕ is found to be proportional to V_0 (see Fig. 4). The slope of the exponential decrease is modified by the transmission of the beam splitter following a $\mathcal{T}_0(1 - \mathcal{T}_0)$ law. Figure 3(b) shows the visibility for different values of V_2 and \mathcal{T}_0 at a magnetic field of 4.6 Tesla. The solid lines are fits to the data using Eq. (1) with $V_\phi = 7.2 \mu\text{V}$ and $T = 25 \text{ mK}$. Clearly, at high bias, there is no V-shape contrary to what has been recently observed in Ref. [8]. Instead, the curves show that the Gaussian approximation is valid. Note that the agreement with our theory is perfect when \mathcal{T}_0 is well defined in our sample. The dispersed data on the edges in Fig. 3(b) coincide to a strong dependence of \mathcal{T}_0 with the voltage applied on $G0$, resulting on an energy dependent transmission \mathcal{T}_0 [8].

We now compare the exponential decrease of the visibility in presence of shot noise with our recent observation that the coherence length of edge states is inversely proportional to the temperature [3]. When $eV_2 \ll k_B T$, the noise is dominated by the Johnson-Nyquist noise $S_{22} = 4k_B T R_Q$. One obtains

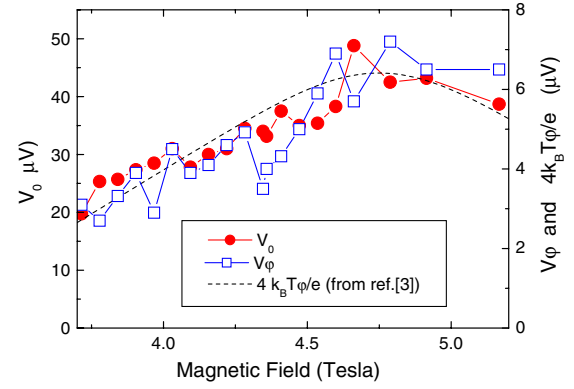


FIG. 4 (color online). V_0 and V_ϕ as a function of the magnetic field. The dashed line is the general behavior of $4k_B T_\phi/e$ (right scale) measured in Ref. [3], on the same sample.

$$\mathcal{V} = \mathcal{V}_0 e^{-T/T_\phi} \quad \text{with} \quad T_\phi^{-1} = \frac{2 \times 8\pi^2 k_B R_Q}{V_0^2} \Delta \nu. \quad (3)$$

Here, the factor 2 arises from the fact that the two arms of the interferometer suffer from a coupling with a noisy IES, instead of one when creating partitioning. From Eqs. (2) and (3), one gets

$$eV_\phi = 4k_B T_\phi. \quad (4)$$

Figure 4, which is our main result, shows that Eq. (4) is in very good agreement with our data. This demonstrates for the first time that thermal noise and coupling between the two edge states are responsible for the finite coherence length measured recently [3]. From the measurements of V_0 and V_ϕ , one can deduce using Eq. (2) that $h\Delta\nu$ varies from ~ 3 to $\sim 7 \mu\text{eV}$ when changing the magnetic field. This value of $h\Delta\nu$ is $\lesssim \max[2k_B T, eV_2]$, which validates our approach of white and Gaussian noise [13].

Figure 4 also brings a valuable point for the understanding of the underlying physics: the proportionality of V_ϕ to V_0 . It can be understood using a simple model where $N_2 = eV_2\tau/h$ ($\tau = L/v_D$, L stands for the interferometer arm length and v_D the drift velocity) electrons in the IES causes a dephasing of $\delta\phi = N_2\varphi_2$ in the OES. Hence, $V_0 = 2\pi h/(e\varphi_2\tau)$ and a Gaussian distribution of N_2 due to partitioning with $\langle \delta N_2^2 \rangle = N_2 \mathcal{T}_0(1 - \mathcal{T}_0)$ leads to $\langle \delta\phi^2 \rangle = \pi\varphi_2^2 \mathcal{T}_0(1 - \mathcal{T}_0)/V_0$ and, therefore, $V_0 = \pi\varphi_2 V_\phi$. Our experiment shows that $\varphi_2 \sim \pi/\sqrt{2}$, independent of the magnetic field. Indeed, this simple approach does not account from the fact that the number of electrons is not a good quantum number in an open system, nor does it gives an independent estimation of φ_2 . Following the work of Seelig and Buttiker [4], we will show that interactions between the edge states, in a mean-field approximation without screening, should lead to $\varphi_2 = \pi$.

Figure 1(b) represents the description adopted here: arm (a), carrying a charge Q_1 , is capacitively coupled through a capacitance C to the IES, carrying a charge Q_2 . The effect

of the electrochemical potential V_2 applied on the IES can be viewed as modifying the potential U_1 felt by electrons in the OES without changing the area S of the MZI [4,10,14]. Fluctuations of U_1 result in fluctuations of the phase $\varphi = \int_0^\tau eU_1 dt/\hbar$. Within this approach, one relates U_1 to V_2 , and the phase noise spectrum S_φ to S_{22} . The total charge on the capacitance is the sum of an emitted charge and a screening charge: $Q_j(\omega) = \nu(\omega)[V_j(\omega) - U_j(\omega)]$, with $\nu(\omega) = iG_Q(1 - e^{i\omega\tau})/\omega$, $x(t) = \int x(\omega)e^{-i\omega t}d\omega$, and $j = 1$ or 2 . Charge neutrality ($Q_1 = -Q_2$) and $U(\omega) = U_2(\omega) - U_1(\omega) = Q_2(\omega)/C$, lead to

$$G_{12} = \frac{dI_1(\omega)}{dV_2(\omega)} = \frac{-i\omega}{C^{-1} + 2\nu(\omega)^{-1}}.$$

Figure 1(c) shows the associated low frequency equivalent circuit: the coupling capacitance C is in series with two relaxation resistances $R_Q/2$ and two quantum capacitances $C_Q = G_Q\tau$. In the zero frequency limit, one gets $U_1 = V_2/(C_Q/C + 2)$, leading to

$$eV_0/h = (2\tau^{-1} + G_Q/C). \quad (5)$$

Note that since both C and τ are proportional to L , V_0 is proportional to L^{-1} . The phase noise $S_\varphi(\omega)$ can then be related to the potential noise $S_{U_1U_1}(\omega)$ by

$$S_\varphi(\omega) = 4\frac{e^2}{\hbar^2}S_{U_1U_1}(\omega)\frac{\sin^2(\omega\tau/2)}{\omega^2}. \quad (6)$$

Equation (6) shows that the total phase fluctuations are given by potential fluctuations integrated over a $\Delta\nu \sim 1/\tau$ bandwidth. Finally, the potential fluctuations are related to the electrochemical fluctuations by

$$|\omega\nu_1(\omega)|^2S_{U_1U_1}(\omega) = |G_{12}(\omega)|^2S_{22}(\omega). \quad (7)$$

We now consider the case of white partition noise $S_{22} = 2eR_QV_2\mathcal{T}_0(1 - \mathcal{T}_0)$ (or white thermal noise $S_{22} = 2 \times 4k_B R_Q T$). Using $\langle \delta\varphi^2 \rangle = \int_0^\infty S_\varphi(\omega)d\omega/2\pi$, one finds

$$V_\varphi^{-1} = \frac{e}{\hbar} \int_0^\infty I(\omega)d\omega, \quad (8)$$

$$\text{with } I(\omega) = \frac{\omega^{-2}}{1 + [\tan(\omega\tau/2)^{-1} + G_Q/C\omega]^2}.$$

It is noteworthy that the dephasing rates described by V_φ and T_φ scale with L^{-1} , as does V_0 . As a consequence, the ratios T_φ/V_0 and V_φ/V_0 should not depend on the size of the interferometer, as confirmed by our observations. In the low frequency limit, $I(\omega) \approx [\omega^2 + (eV_0/h)^2]^{-1}$ which leads to

$$V_0 = \pi^2 V_\varphi. \quad (9)$$

Numerically, we find that the equality (9) stands for all values of C/C_Q within the [0.03, 0.3] expected range [3]. Although our approach naturally explains why $V_\varphi \propto V_0$ and gives the correct order of magnitude, it overestimates

the dephasing by a factor of ~ 1.4 . This discrepancy can be eliminated by including the screening by the compressible regions of the 2DEG, which tend to shortcircuit high frequency fluctuations [15]. The variation of V_0 across the $\nu = 2$ plateau with a fairly constant V_0/V_φ most probably results from a variation of the effective trajectory length with B , due to the disorder, as all the microscopic parameters (namely, C_Q , C and the capacitance to ground C_0) scales with the length. However, one cannot totally exclude a more subtle variation of the microscopic structure of the edge states, leading to variations of the coupling and of the screening while keeping V_0/V_φ constant. Indeed, an independent measurement of τ would shed light on this. Last, we would like to stress that, while all of our observations are very well explained by Gaussian fluctuations, in very similar systems with a similar inter edge coupling, a different behavior has been reported in [8], which was attributed to non-Gaussian noise. The reason for such difference remains puzzling.

To conclude, we have shown that the coherence length of the edge states at filling factor 2 is limited by the Johnson-Nyquist noise. Changing the magnetic field makes it possible to modify the coupling between the edge states and thus modifies the coherence length. Our results are well described by a mean-field approach that relates the phase randomization to the fluctuations of the electrostatic potential in the interferometer arms.

The authors would like to thank Markus Buttiker for fruitful discussions.

-
- [1] Y. Ji *et al.*, Nature (London) **422**, 415 (2003).
 - [2] I. Neder *et al.*, Nature (London) **448**, 333 (2007).
 - [3] P. Roulleau *et al.*, Phys. Rev. Lett. **100**, 126802 (2008).
 - [4] G. Seelig and M. Buttiker, Phys. Rev. B **64**, 245313 (2001).
 - [5] S. E. Barrett, Phys. Rev. Lett. **74**, 5112 (1995).
 - [6] T. Martin and S. Feng, Phys. Rev. Lett. **64**, 1971 (1990).
 - [7] D. C. Dixon *et al.*, Phys. Rev. B **56**, 4743 (1997).
 - [8] I. Neder *et al.*, Nature Phys. **3**, 534 (2007).
 - [9] P. Roulleau *et al.*, Phys. Rev. B **76**, 161309 (2007).
 - [10] A. Stern, Y. Aharonov, and Y. Imry, Phys. Rev. A **41**, 3436 (1990).
 - [11] T. Martin and R. Landauer, Phys. Rev. B **45**, 1742 (1992).
 - [12] M. Büttiker, Phys. Rev. B **46**, 12485 (1992).
 - [13] This can lead to a small deviation between experiments and our theory at the lowest temperature (20 mK) when $eV_2 \leq 2k_B T$.
 - [14] D. Rohrich *et al.*, Phys. Rev. Lett. **98**, 096803 (2007).
 - [15] The screening can be modeled by two additional capacitances C_0 connecting the edges states to the ground. This model reproduces the observed constant ratio V_0/V_φ within 5% for $C/C_Q \in [0.03, 0.3]$, provided that $C_0 \approx 0.5(CC_Q)^{1/2}$. A more detailed study will be published elsewhere.